ACS APPLIED MATERIALS & INTERFACES

Research Article

www.acsami.org

Multifunctional Free-Standing Membrane from the Self-assembly of Ultralong MnO_2 Nanowires

Bang Lan,[†] Lin Yu,*[,†] Ting Lin,[†] Gao Cheng,[†] Ming Sun,[†] Fei Ye,[†] Qingfeng Sun,[‡] and Jun He[†]

[†]School of Chemical Engineering and Light Industry, Guangdong University of Technology, Guangzhou 510006, People's Republic of China

[‡]Key laboratory of Bio-based Material Science and Technology, Ministry of Education, Northeast Forestry University, Harbin 150040, People's Republic of China

Supporting Information

ABSTRACT: In this work, we report the preparation of a free-standing membrane with strong mechanical stability and flexibility through a facile vacuum filtration approach. A field-emission scanning electron microscopy image demonstrates that the membrane composed of MnO_2 nanowires is 50 nm in width and up to 100 μm long and the nanowires are assembled in parallel into bundles. A possible formation mechanism for the ultralong nanowires and the free-standing membrane has been proposed. Meanwhile, the properties of the membrane could be controlled by incorporating different materials to achieve composite membranes. In order to demonstrate the broad applicability of the MnO_2 membrane, we fabricate a variety of composite membranes exhibiting various novel properties including magnetism and reversibly switchable wettability between hydrophilicity and hydrophobicity through various material modification, including $CoFe_2O_4$ nanoparticles and organic triethoxy(octyl)silane. Furthermore, the free-standing membrane could also simultaneously be functionalized with two materials, which reveal multiple properties. The synthesis method of a free-standing MnO_2 membrane is simple and environmentally friendly, and it is easily scalable for industry. These composite membranes constitute a significant contribution to advanced technology.

KEYWORDS: *MnO_2, multifunctional free-standing membrane, ultralong nanowires*

INTRODUCTION

In the past decades, one-dimensional (1D) nanomaterials such as nanorod, nanotube, nanobelt, and especially ultralong nanowires have attracted intensive attention because of their potential applications in supercapacitors,[1] lithium-ion batteries,[2] gas sensors,[3] photodetection,[4] catalysis,[5] and so on.[6,7] However, it is frequently necessary to assemble 1D nanomaterials into macroscopic architectures [e.g., a two-dimensional (2D) membrane], for achieving practical applications.[8−12] Even more important, the macroscopic assemblies are expected to possess cumulative properties of individual 1D nanomaterials and exhibit novel characteristic in various fields.

It is of great interest to assemble 1D nanomaterials into 2D macroscopic inorganic membrane because of their unique advantages such as low weight, high permeability, high surface area, and large porosity.[13−16] Various techniques and approaches have been developed to prepare ultralong nanowire membranes. A common technology is the Langmuir−Blodgett (LB) approach, which is substrate-based to assemble nanofibers or ultralong nanowires into membranes with oriented and periodic nanostructures.[9,17] However, as for the LB approach, the surface of the 1D nanomaterials must be functionalized with hydrophobic ligands and complicated operating processes with special equipments are required, which greatly restricts their industry-wide application. Recently, Yu et al.[18] reported that silver nanowires can be spontaneously assembled at the three interfaces to form an ordered free-standing membrane. This method is without the need for hydrophobic treatment, but the prepared sample is also substrate-based. Another technique commonly used to form a nanowire membrane is vacuum filtration. Recently, Peng and Ichinose[19] fabricated an ultrathin membrane of MnOOH nanofibers by filtering the dispersed solution on a polycarbonate membrane filter with narrow pore-size distributions. Yu and co-workers[20,21] developed a hydrothermal carbonization process to synthesize an ultralong carbon nanofiber membrane using expensive tellurium nanowires acting as templates under mild conditions. However, the special equipment and expensive templates involved in these syntheses dramatically hinder large-scale production of the membranes for practical application. Moreover, this vacuum filtration method requires nanowires with very high aspect ratio and good dispersion in the solvents, which resulted in fewer membranes from 1D nanomaterials that have been reported using this method.

Received: May 11, 2013
Accepted: July 1, 2013
Published: July 1, 2013

The blending of the different components into a single structure often results in composite materials with combined and/or enhanced properties originating from individual components, and, more significantly, new phenomena and functionalities that are not possible with the individual components alone can be induced in the composite materials.[22] In particular, the property of the membrane can basically be related to both the chemical composition and surface structure of the nanowires. The 2D membrane can further be functionalized by the incorporation of inorganic and/or organic additives on the surface of the nanowires.[15,23,24] For example, Peng and co-workers[23] developed a simple method to fabricate ultrathin films that were composed of positively charged cadmium hydroxide nanostrands of only 1.9 nm diameter and micrometers in length and negatively charged functional nanoparticles, proteins, or dye molecules. Yu and co-workers[24] found that a carbon nanofiber membrane could be functionalized with various nanomaterials such as, Fe_3O_4, TiO_2, Ag, Au, etc., which reveal multifunctional properties including magnetism, antibiofouling, and catalytic ability. Suib and co-workers[15] have fabricated a hydrophobic MnO_2 membrane with improved properties for oil/water separation. However, their synthesis conditions are harsh. These above methods have their own advantages, but the membranes are usually functionalized with only one kind of materials. It is also attractive to integrate two or more kinds of materials into a single membrane to prepare a multifunctional membrane with advanced properties.

Herein, we report a new class of membranes consisting of highly uniform ultralong MnO_2 nanowires that can be synthesized under mild conditions. The ultralong nanowires can be readily self-assembled into a free-standing membrane through vacuum filtration because of its extraordinary flexibility and good dispersion in water. In comparison with conventional membranes, the membrane reported herein could easily be fully functionalized by applying the bottom-up strategy of the surface modification of the nanowires. Important, the free-standing membrane could also simultaneously be functionalized with two different kinds of materials, such as organic triethoxy(octyl)silane and inorganic nanoparticles $CoFe_2O_4$, which integrate the features of different materials.

EXPERIMENTAL SECTION

Chemicals. All of the chemicals were of analytical grade and were used as received without further purification. $MnSO_4{\cdot}H_2O$, $KClO_3$, CH_3COOK, CH_3COOH, $FeCl_3{\cdot}6H_2O$, CH_3COONa, $Co(CH_3COO)_2{\cdot}4H_2O$, diethylene glycol (DEG), ethanol, toluene, and triethoxy(octyl)silane (TEOOS) were all supplied by Guangzhou Chemical Reagent Company.

Synthesis. *Synthesis of MnO_2 Nanowires.* In a typical synthesis, 1 mmol of $MnSO_4{\cdot}H_2O$, 1.75 mmol of $KClO_3$, and 1.75 mmol of CH_3COOK were dissolved in 15 mL of distilled water. When the solution was clarified, 0.8 mL of CH_3COOH was added to the above solution under continuous stirring. The resulting solution was transferred into a 25 mL Teflon-lined stainless steel autoclave and maintained at 160 °C for 8 h and then naturally cooled to room temperature. The precipitates were collected by vacuum filtration with common filter paper, washed several times with distilled water and absolute ethanol, respectively, and dried at 60 °C for 4 h. Then, the free-standing MnO_2 membrane can be prepared.

Synthesis of Magnetic $CoFe_2O_4$. The synthesis of $CoFe_2O_4$ used a protocol similar to that reported.[25] $FeCl_3{\cdot}6H_2O$ and $Co(CH_3COO)_2{\cdot}4H_2O$ in stoichiometric ratio (2:1), together with sodium acetate with a mole ratio of 3.5 (CH_3COO/metal), were added to a given volume of DEG. The total metal content was 0.3 mol. The mixture was then heated to its boiling point and refluxed for 5 h. After cooling to room temperature, the particles were separated by centrifugation, washed with ethanol and acetone, and then dried in air at 60 °C.

Preparation of a Magnetic Membrane. A total of 0.1 g of $CoFe_2O_4$ was dispersed into 100 mL of absolute ethanol and sonicated for 60 min. Then 0.2 g of as-prepared MnO_2 nanowires was added to the above solution under stirring for 4 h. The product was collected by vacuum filtration, washed with absolute ethanol, and then dried at 60 °C for 2 h.

Preparation of a Hydrophobic Membrane. The hydrophobic MnO_2 membrane was prepared according to a modified method of Cargnello et al.[26] The as-prepared MnO_2 nanowires (0.2 g) were sonicated in 20 mL of toluene for 1 h, followed by the addition of 1 mL of TEOOS. The resulting solution was refluxed at 60 °C for 6 h, and the product was collected by vacuum filtration, washed with absolute ethanol, and then dried at 60 °C for 2 h.

Preparation of a Multifunctional Membrane. The preparation of a multifunctional membrane is similar to that of a hydrophobic membrane except that a magnetic MnO_2 membrane is substituted for MnO_2.

Characterization. The products were characterized with a Bruker D8-advance X-ray diffractometer with Cu Kα radiation (λ = 1.5418 Å, 40 kV, and 40 mA) at a scan rate of 4°/min. The field-emission scanning electron microscopy (FESEM) images were recorded on a ZEISS Ultra 55. The transmission electron microscopy (TEM) images, electron diffraction patterns, and high-resolution TEM (HRTEM) images were recorded on a JEOL JEM-2100HR at an acceleration voltage of 200 kV. The magnetic properties of the samples were investigated using a superconducting quantum interface device (SQUID) magnetometer (Quantum Design MPMS-XL-7). The contact angle (CA) was determined by the sessile drop method using a DataPhysics OCA20 (Germany) contact angle measuring device, which has a computer-controlled video camera to photograph the material and an electronic syringe to drip fluid onto the membrane.

RESULTS AND DISCUSSION

Preparation of Ultralong MnO_2 Nanowires and Membrane. X-ray diffraction (XRD) was used to investigate the phase purity of the solid. The XRD pattern of the synthesized free-standing MnO_2 membrane is shown in Figure 1. All of the peaks can be indexed as tetragonal α-MnO_2 (space group: $I4/m$) with cell parameters a = 9.78 Å and c = 2.86 Å, which are consistent with the values of the standard card (PDF 81-1947). No other crystalline phase was shown in Figure 1, indicating the high purity of the product. The inset of Figure 1 is typical of the α-MnO_2 structure, which contains a well-defined 2 × 2 tunnel structure with a pore size of about 4.6 Å

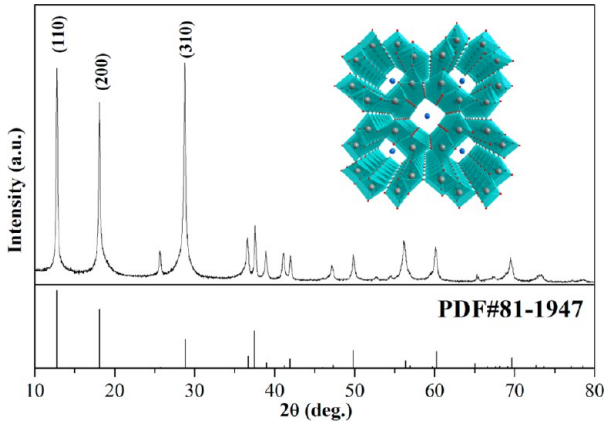

Figure 1. XRD pattern of α-MnO_2. Inset: representation of the crystal structure for α-MnO_2.

dx.doi.org/10.1021/am401774r | ACS Appl. Mater. Interfaces 2013, 5, 7458−7464

and is composed of double chains of edge-shared MnO_6 octahedra and corner sharing of double chains. Manganese atoms in the octahedra are mainly presented as Mn^{4+} and Mn^{3+}, and that countercation K^+ partially occupies the tunnel to balance and stabilize the structure.[27]

The SEM image in Figure 2a shows the general morphology of the MnO_2 membrane. It can be seen that the membrane

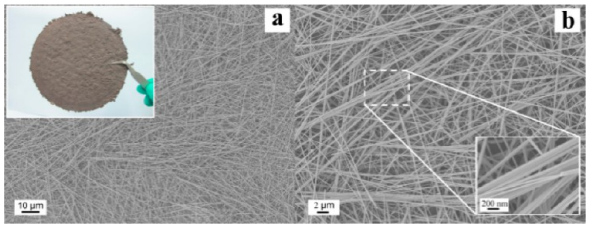

Figure 2. FESEM images of the membrane: (a) overall view of the membrane; (b) higher magnification of the membrane. Insets: photographs of the free-standing membrane.

consists of abundant randomly oriented ultralong nanowires with lengths larger than 100 μm. The nanowires interconnect with each other to form a mesh structure with high porosity and flexibility. The inset in Figure 2a is an optical image of the free-standing MnO_2 membrane. The size of the membrane can be varied in a controllable manner through control of the size of the substrate and the concentration of the MnO_2 nanowires. For example, a free-standing membrane of 5 cm and 10 cm diameter has been obtain (see the Supporting Information, Figure S1a,b). The membrane also can be cut and curled like a piece of paper (see the Supporting Information, Figure S1c,d). The high-magnification SEM image in Figure 2b reveals that the network architectures originate from intertwined nanowires and nanowire bundles. The nanowire bundles (see the inset in Figure 2b) are made up of ultralong nanowires, which have typical diameters of about 50 nm. The BET surface area of the synthesized MnO_2 membrane is 17 m^2/g.

The crystal structure and growth direction of the nanowire were investigated by HRTEM analysis, and the corresponding selected-area electron diffraction (SAED) pattern is given. The TEM image of a typical individual MnO_2 nanowire is shown in Figure 3a. The SAED pattern and HRTEM image taken from the white squares in Figure 3a are shown in Figure 3b,c. The SAED pattern (Figure 3b) can be indexed in the tetragonal of α-MnO_2, which is consistent with the XRD results. The three

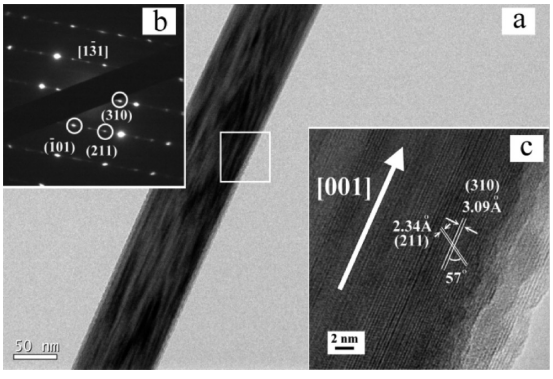

Figure 3. (a) TEM image of a typical α-MnO_2 nanowire with its SAED pattern in part b. (c) HRTEM image from the white square indicated in part a.

bright spots from the circle correspond to (−101), (211), and (310). The zone axis is [1−31]. As evidenced by the HRTEM image in Figure 3c, the distance between the adjacent lattice fringes that run parallel to the nanowire is around 3.09 Å, which can be assigned as the interplane distance of (310) planes of α-MnO_2 structure. Another distance between the fringes is d = 2.34 Å, which corresponds to the interplane distance of (211) planes. The angle between the two planes is 57°. Therefore, the ultralong nanowires grow along the [001] direction.

Three possible reasons are proposed to explain the formation of the ultralong nanowires and nanowire bundles. First, if the concentration of carbonyl groups from CH_3COOH in the reaction bath is sufficiently high, it could form bonds with the surface OH groups on the manganese oxide materials.[28−30] The absorbed carbonyl groups through steric effects hinder the chemical reactive sites of the lateral nanowires. Because the crystallographic structure of α-MnO_2 belongs to the tetragonal system, it can preferentially grow along the c axis. Second, from the viewpoint of thermodynamics, the difference of the redox potentials between ClO_3^-/Cl^- (1.45 V) and Mn^{4+}/Mn^{2+} (1.23 V) is about 0.22 V, resulting in appropriate redox reaction and optimal growth rates. A larger difference of the standard electrode potentials can cause the quick formation of the small nuclei of MnO_2 and, subsequently, limit particle growth due to exhaustion of the reactants.[31] A smaller difference of the standard electrode potentials will make the reaction mild and slow, resulting in the formation of a well-ordered dendritic structure, as proposed by Suib et al.[32] Third, Ostwald ripening is considered. The inset of Figure 2b clearly reveals that the primary nanowires aggregate along the lateral direction to form nanowire bundles. TEM images in Figure S2 in the Supporting Information also reveal the laterally oriented attachment of nanowires on a preferential plane. According to the previous results,[33] the nanowires were easy to attach to each other to form bundles under an acidic medium. Therefore, steric effects, appropriately different redox potentials, and Ostwald ripening contribute to the formation of ultralong nanowires and nanowire bundles.

As for the possible mechanism of the self-assembly of MnO_2 nanowires into a free-standing membrane, the hydrogen bonding and flexibility of ultralong nanowires are considered to play a key role. Under the synthesis conditions, the H_2O molecules could act not only as the solvent but also as an excellent hydrogen-bond donor/acceptor, which provide the driving force of hydrogen bonding for the self-assembly of ultralong nanowires into a free-standing membrane.[34,35] In our case, OH on the surface of manganese oxide could form hydrogen bonds with H_2O.[36,37] The ultralong nanowires (more than 100 μm) entangle with each other, and the hydrogen bonds serve as the bonding force during entangling. Finally, this self-assembled free-standing MnO_2 membrane is obtained.

Magnetic Membrane Modified by $CoFe_2O_4$ Nanoparticles. The free-standing membrane is easily functionalized by incorporating nanoparticles to achieve novel properties. In our study, the free-standing MnO_2 membrane is modified by magnetic nanoparticles that exhibit superior magnetic properties as an example. The magnetic $CoFe_2O_4$ nanoparticles were synthesized through hydrolysis in a polyol medium.[25] All of the peaks of the XRD pattern in Figure S3 in the Supporting Information could be perfectly indexed to the pure cubic spinel crystal structure of $CoFe_2O_4$ (PDF 22-1086). Subsequently, magnetic $CoFe_2O_4$ nanoparticles were grafted onto the surface of MnO_2 nanowires after stirring in ethanol for 4 h. The XRD

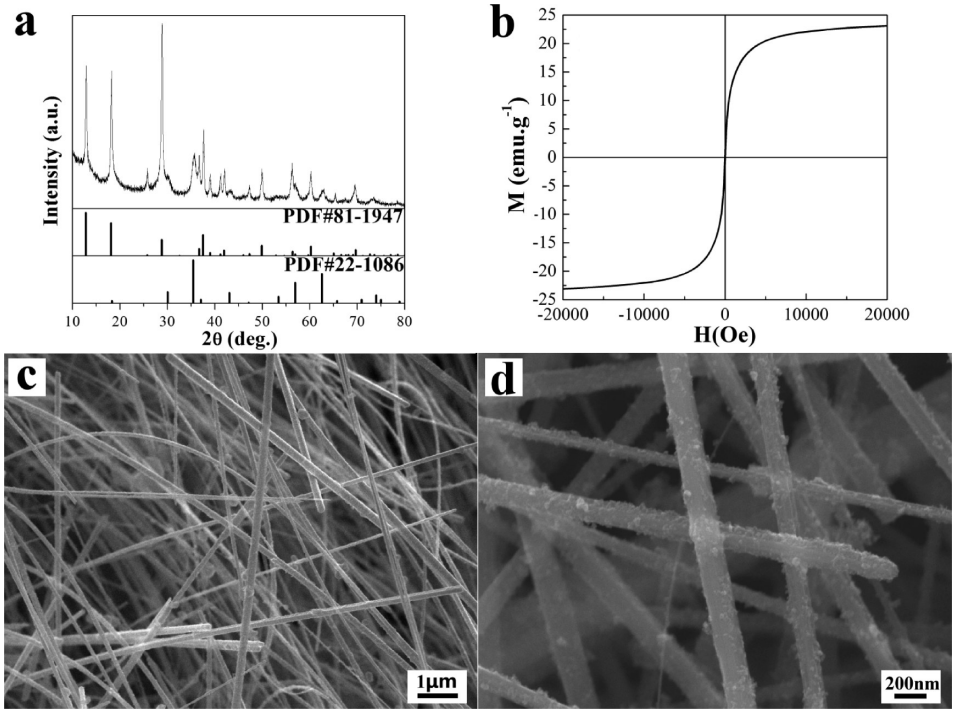

Figure 4. Phase, magnetic, and morphology characterization of the magnetic membrane: (a) XRD pattern of the magnetic membrane; (b) room temperature magnetic hysteresis loop of the magnetic membrane; (c and d) SEM images of the magnetic membrane.

pattern of the MnO_2 membrane modified by $CoFe_2O_4$ is shown in Figure 4a. Compared with the XRD pattern of a pure MnO_2 membrane (Figure 1), two additional peaks at 35° and 62° marked as $CoFe_2O_4$ (PDF 22-1086) were observed. No remarkable shift in the diffraction peak was detected. Figure 4c presents the SEM image of the magnetic MnO_2 membrane. It can be seen from the high-magnification SEM image (Figure 4d) that the surface of MnO_2 nanowires is partially covered by $CoFe_2O_4$ nanoparticles. Energy-dispersive X-ray spectroscopy (EDX) analysis further confirms the existence of potassium, manganese, iron, cobalt, and oxygen elements (see the Supporting Information, Figure S4). The magnetic properties of the as-prepared membrane were measured using a SQUID magnetometer at room temperature with an applied field of $-20\ \text{kOe} \leq H \leq 20\ \text{kOe}$. The magnetization curve in Figure 4b shows that the magnetic membrane has a saturation magnetization of 23.0 emu/g. The closed hysteresis loop indicated that the membrane retains the superparamagnetic characteristic of the $CoFe_2O_4$ nanoparticles. The membrane exhibited remarkable magnetism. Video S1 in the Supporting Information shows that the prepared magnetic membrane can be attracted by a simple household magnet without any apparent damage.

The formation mechanism of $CoFe_2O_4$-nanoparticle-modified MnO_2 nanowires can be attributed to the dipole interaction and abundance of hydrogen bonding. First, as a paramagnetic substance, MnO_2 can couple with superparamagnetic $CoFe_2O_4$ nanoparticles through magnetic dipole−dipole interactions.[38,39] The dipole interaction can cause the superparamagnetic $CoFe_2O_4$ nanoparticles to be grafted onto the surface of MnO_2 nanowires more easily. Moreover, because the $CoFe_2O_4$ nanoparticles were synthesized in the polyol soultion, the surface of $CoFe_2O_4$ nanoparticles are covered by a large number of OH groups.[40] Meanwhile, the MnO_2 nanowires are also covered by OH groups. Therefore, the $CoFe_2O_4$ nanoparticles can be grafted onto the surface of MnO_2 nanowires through hydrogen bonding. As a result, a novel magnetic membrane can be successfully prepared in a facile way. Furthermore, it can be inferred that other functional inorganic materials, such as Ag, Pt, and Fe_3O_4, synthesized in the polyol medium can also rapidly be grafted onto the surface of MnO_2 nanowires, resulting in the membrane exhibiting other extraordinary properties.

Reversible Wetting Membrane Modified by TEOOS. TEOOS has usually been used to modify the surface wettability of the materials.[26] In our study, the free-standing MnO_2 membrane modified by TEOOS can show reversible wettability between hydrophilicity and hydrophobicity. Because the surface of MnO_2 nanowires contains a large number of OH groups, the silanol groups formed by hydrolysis of TEOOS can easily react with OH groups of manganese oxide to form bonds of Si−O−Mn, resulting in a layer of hydrophobic alkyl groups covering the surface of nanowires. XPS analysis was used to identify the surface elemental composition of the as-synthesized membrane. The survey spectra (see the Supporting Information, Figure S5a) indicate that the sample contains manganese, oxygen, potassium, and silicon elements. The peak at a binding energy of 101.93 eV representing Si 2p is consistent with the reported values of silicon[41] (see the Supporting Information, Figure S5b), which may indicate that the main silicon is Si^{4+}. Although the silicon content is only 1.37%, the modified membrane becomes hydrophobic. When the water droplet was deposited on the pristine membrane, it immediately spread out and penetrated into the membrane as a consequence of the favorable interactions with the OH groups on the surface. By contrast, when the water droplet was deposited on the TEOOS modified membrane, it was repulsed (see the Supporting Information, video S2).

The reversible wettability of the functional membrane between hydrophobicity and hydrophilicity was evaluated by the water CA measurement. Figure 5a shows a spherical water

dx.doi.org/10.1021/am401774r | ACS Appl. Mater. Interfaces 2013, 5, 7458−7464

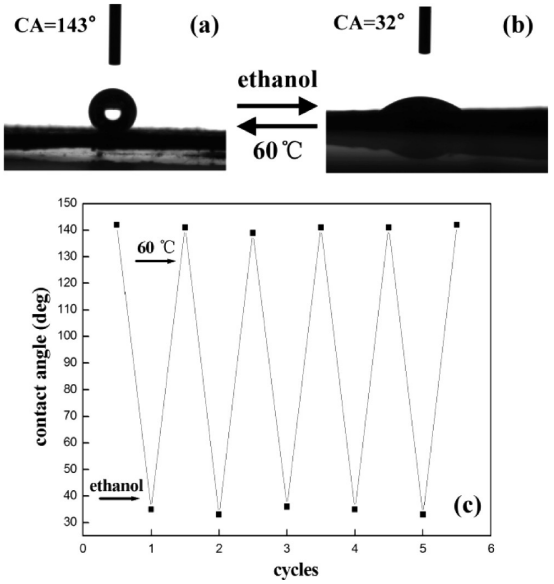

Figure 5. Photographs of the water droplet shape on the membrane before (a) and after (b) treatment with ethanol. (c) Reversible hydrophobic-to-hydrophilic transformation of the as-prepared membrane under alternation of an ethanol treatment and 60 °C heating.

droplet with a water CA of 143° on the TEOOS modified membrane. After a drop of ethanol was added onto the membrane, the water droplet quickly penetrated into the membrane, resulting in a water CA of about 32° in Figure 5b. The results indicate that the wettability of the as-prepared membrane varied from hydrophobicity to hydrophilicity. Further experimental evidence demonstrate that the hydrophobicity of the membrane can recover again after heat-treatment of the membrane in an oven at 60 °C for 5 min. When treated by ethanol at same place and heat-treatment alternately, the wettability of membrane could be switched between hydrophilicity and hydrophobicity. Only slight change in water CAs was observed in each switching (five times for the study show in Figure 5c), indicating that the membrane can be tuned continuously and reversibly from hydrophobicity to hydrophilicity in a facile way.

The reversible features are quite different from the traditional commercial membranes, which usually are impossible to be tuned continuously and reversibly from hydrophobicity to hydrophilicity. To thoroughly understand the reversible transformation of the membrane between hydrophobicity and hydrophilicity, the surface composition, which is the main factor governing the surface wettability, was considered. Because the surface of MnO_2 nanowires is coated with a layer of silicone, the hydrophobic alkyl group of the silicone is responsible for the hydrophobicity.[15] However, when the hydrophobic membrane was treated with ethanol, a dense ethanol layer was covered on the surface of the membrane. Ethanol molecules serve not only as hydrogen-bond donors for the surface of OH groups but also as hydrogen-bond acceptors for the water molecules, which make the water penetrate into the membrane smoothly through the similarity principle and hydrogen-bonding interaction.[37] Several kinds of organic solvents were used in the experiment, and the results show that polar organic solvents such as methanol and acetone have the same effect as ethanol, allowing the water to penetrate into the membrane, while when nonpolar solvents such as cyclohexane and tetrachloromethane were added to the membrane, the CA remained 138° (see the Supporting Information, Figure S6), revealing that the membrane remained hydrophobic.

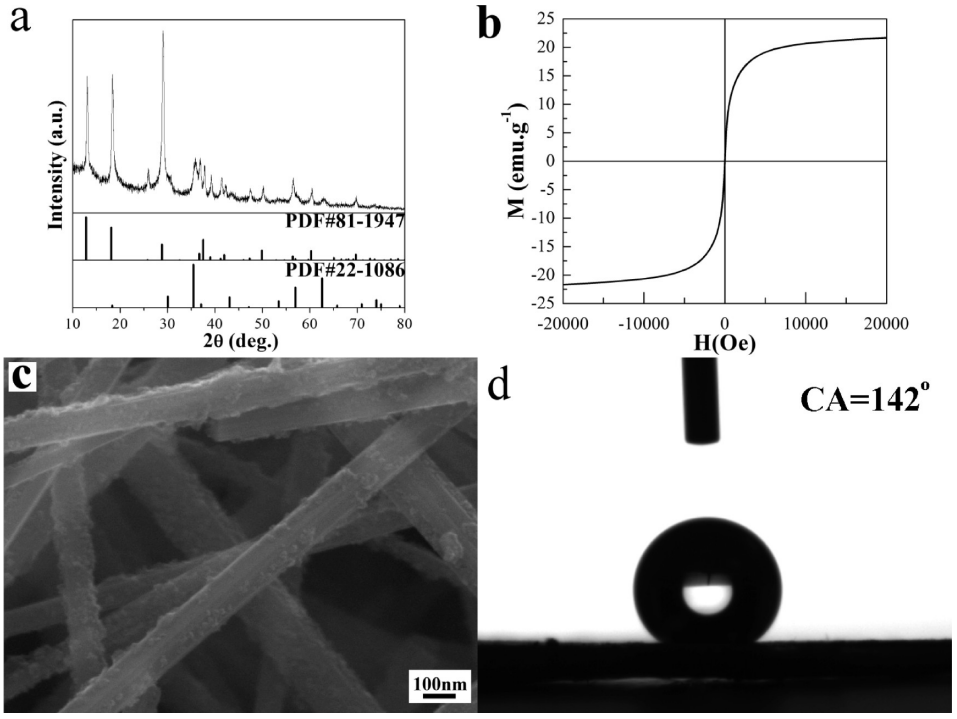

Figure 6. Phase, morphology, magnetic, and wetting characterization of the multifunctional membrane: (a) XRD pattern of the multifunctional membrane; (b) room temperature magnetic hysteresis loop of the multifunctional membrane; (c) SEM image of the multifunctional membrane; (d) photograph of the water droplet shape on the multifunctional membrane.

In short, we successfully prepared a hydrophobic membrane by using TEOOS modification. The membrane can exhibit reversible wettability between hydrophilicity and hydrophobicity by incorporating a hydrophobic alkyl group and through the addition of polar solvents. It can be inferred that other organic functional groups, such as −COOH, $-NH_2$, and −SH, can also modify the MnO_2 membrane through different silanes to achieve other novel properties.

Multifunctional Membrane. On the basic of the above experimental results and standpoints, a novel multifunctional membrane by incorporating $CoFe_2O_4$ nanoparticles and TEOOS could be designed and prepared in this study. XRD patterns in Figure 6a reveal that the membrane is composed of α-MnO_2 (PDF 81-1947) and the coexistence of $CoFe_2O_4$ (PDF 22-1086). No additional peaks or peak shifts are found in the XRD pattern, indicating that the crystalline phase does not change following by the incorporation of modified TEOOS. Figure 6c shows that abundant $CoFe_2O_4$ nanoparticles are uniformly dispersed on the surface of MnO_2 nanowires, and even after the ultrasonic treatment of the sample, $CoFe_2O_4$ nanoparticles still stick closely to the surface of MnO_2 nanowires. Compositional analysis of the multifunctional membrane by EDX in Figure S7 in the Supporting Information reveals the presence of potassium, manganese, cobalt, iron, silison, and oxygen elements. Figure 6b shows the magnetization curve of the multifunctional membrane. It can be seen from the room temperature hysteresis loop that the saturation magnetization is 21.6 emu/g, only a slight change in the saturation magnetization after TEOOS modification. The result of water CA measurements is present in Figure 6d. The membrane surface shows a water CA of 142°. The water droplets roll off the surface easily. Video S3 in the Supporting Information shows that the membrane exhibits both magnetism and hydrophobicity. Notably, the membrane is extremely stable, and the properties can remain unaltered at ambient temperature for more than 3 months.

CONCLUSION

In summary, we have successfully taken advantage of the hydrogen bonding and flexibility of ultralong MnO_2 to fabricate a free-standing membrane through a simple vacuum filtration technique. We also demonstrate that the membrane can be modified by various functional additives, such as inorganic nanoparticles $CoFe_2O_4$ and organic TEOOS, with desirable properties, including magnetism and reversible wettability between hydrophilicity and hydrophobicity. Particularly, the membrane could be simultaneously functionalized with two or more kinds of materials, resulting in a multifunctional composite membrane. The present free-standing MnO_2 membrane could be modified by other functional materials, which enables the creation of multifunctional composite membranes with improved properties and practical applications such as oil/water separation, separation of biomacromolecules, and heterogeneous catalysis.

ASSOCIATED CONTENT

Supporting Information

Photographs of the free-standing membrane (Figure S1), TEM images of the ultralong nanowire (Figure S2), XRD pattern of $CoFe_2O_4$ (Figure S3), EDX spectrum of the magnetic membrane (Figure S4), XPS spectrum of the hydrophobic membrane (Figure S5), photographs of water droplet shape on the membrane with different solvent treatments (Figure S6), EDX spectrum of a multifunctional membrane (Figure S7), and three videos. This material is available free of charge via the Internet at http://pubs.acs.org.

AUTHOR INFORMATION

Corresponding Author

*E-mail: gych@gdut.edu.cn.

Notes

The authors declare no competing financial interest.

ACKNOWLEDGMENTS

This work was financially supported by the Natural Science Foundation of Guangdong Province (Grants 10251009001000003 and S2012010009680), Scientific Program of Guangzhou (Grant 2010Z1-E061), Scientific Program of Guangdong Province (Grant 2012A030600006), Fund of Higher Education of Guangdong Province (Grant cgzhzd1104), and the 211 Project of Guangdong Province.

REFERENCES

(1) Jiang, H.; Zhao, T.; Ma, J.; Yan, C.; Li, C. *Chem. Commun.* **2011**, *47* (4), 1264−1266.
(2) Lee, H. W.; Muralidharan, P.; Ruffo, R.; Mari, C. M.; Cui, Y.; Kim, D. K. *Nano Lett.* **2010**, *10* (10), 3852−3856.
(3) Liu, J.; Wang, X.; Peng, Q.; Li, Y. *Adv. Mater.* **2005**, *17* (6), 764−767.
(4) Zhai, T.; Li, L.; Ma, Y.; Liao, M.; Wang, X.; Fang, X.; Yao, J.; Bando, Y.; Golberg, D. *Chem. Soc. Rev.* **2011**, *40* (5), 2986−3004.
(5) Xie, X.; Li, Y.; Liu, Z.; Haruta, M.; Shen, W. *Nature* **2009**, *458* (7239), 746−749.
(6) Xia, Y.; Yang, P.; Sun, Y. G.; Wu, Y. Y.; Mayers, B.; Gates, B.; Yin, Y. D.; Kim, F.; Yan, Y. Q. *Adv. Mater.* **2003**, *15* (5), 353−389.
(7) Burda, C.; Chen, X.; Narayanan, R.; El-Sayed, M. A. *Chem. Rev.* **2005**, *105* (4), 1025−1102.
(8) Liang, H.-W.; Guan, Q.-F.; Chen, L.-F.; Zhu, Z.; Zhang, W.-J.; Yu, S.-H. *Angew. Chem., Int. Ed.* **2012**, *51* (21), 5101−5105.
(9) Liu, J.-W.; Liang, H.-W.; Yu, S.-H. *Chem. Rev.* **2012**, *112* (8), 4770−4799.
(10) Liu, J.-W.; Xu, J.; Liang, H.-W.; Wang, K.; Yu, S.-H. *Angew. Chem., Int. Ed.* **2012**, *51* (30), 7420−7425.
(11) Zhang, C.-L.; Lv, K.-P.; Hu, N.-Y.; Yu, L.; Ren, X.-F.; Liu, S.-L.; Yu, S.-H. *Small* **2012**, *8* (19), 2936−2940.
(12) Wu, Z.-Y.; Li, C.; Liang, H.-W.; Chen, J.-F.; Yu, S.-H. *Angew. Chem., Int. Ed.* **2013**, *52* (10), 2925−2929.
(13) Gu, G.; Schmid, M.; Chiu, P. W.; Minett, A.; Fraysse, J.; Kim, G. T.; Roth, S.; Kozlov, M.; Munoz, E.; Baughman, R. H. *Nat. Mater.* **2003**, *2* (5), 316−319.
(14) Endo, M.; Muramatsu, H.; Hayashi, T.; Kim, Y. A.; Terrones, M.; Dresselhaus, M. S. *Nature* **2005**, *433* (7025), 476−476.
(15) Yuan, J.; Liu, X.; Akbulut, O.; Hu, J.; Suib, S. L.; Kong, J.; Stellacci, F. *Nat. Nanotechnol.* **2008**, *3* (6), 332−336.
(16) Wang, Y.; Du, G.; Liu, H.; Liu, D.; Qin, S.; Wang, N.; Hu, C.; Tao, X.; Jiao, J.; Wang, J.; Wang, Z. L. *Adv. Funct. Mater.* **2008**, *18* (7), 1131−1137.
(17) Liu, J.-W.; Zhu, J.-H.; Zhang, C.-L.; Liang, H.-W.; Yu, S.-H. *J. Am. Chem. Soc.* **2010**, *132* (26), 8945−8952.
(18) Shi, H.-Y.; Hu, B.; Yu, X.-C.; Zhao, R.-L.; Ren, X.-F.; Liu, S.-L.; Liu, J.-W.; Feng, M.; Xu, A.-W.; Yu, S.-H. *Adv. Funct. Mater.* **2010**, *20* (6), 958−964.
(19) Peng, X.; Ichinose, I. *Adv. Funct. Mater.* **2011**, *21* (11), 2080−2087.
(20) Qian, H.-S.; Yu, S.-H.; Luo, L.-B.; Gong, J.-Y.; Fei, L.-F.; Liu, X.-M. *Chem. Mater.* **2006**, *18* (8), 2102−2108.
(21) Liang, H.-W.; Wang, L.; Chen, P.-Y.; Lin, H.-T.; Chen, L.-F.; He, D.; Yu, S.-H. *Adv. Mater.* **2010**, *22* (42), 4691−4695.
(22) Huang, X.; Li, J.; Fu, H. *J. Am. Chem. Soc.* **2000**, *122* (36), 8789−8790.

(23) Peng, X.; Jin, J.; Ericsson, E. M.; Ichinose, I. *J. Am. Chem. Soc.* **2007**, *129* (27), 8625−8633.
(24) Liang, H.-W.; Zhang, W.-J.; Ma, Y.-N.; Cao, X.; Guan, Q.-F.; Xu, W.-P.; Yu, S.-H. *ACS Nano* **2011**, *5* (10), 8148−8161.
(25) Ammar, S.; Helfen, A.; Jouini, N.; Fievet, F.; Rosenman, I.; Villain, F.; Molinie, P.; Danot, M. *J. Mater. Chem.* **2001**, *11* (1), 186−192.
(26) Cargnello, M.; Jaén, J. J. D.; Garrido, J. C. H.; Bakhmutsky, K.; Montini, T.; Gámez, J. J. C.; Gorte, R. J.; Fornasiero, P. *Science* **2012**, *337* (6095), 713−717.
(27) Ding, Y. S.; Shen, X. F.; Sithambaram, S.; Gomez, S.; Kumar, R.; Crisostomo, V. M. B.; Suib, S. L.; Aindow, M. *Chem. Mater.* **2005**, *17* (21), 5382−5389.
(28) Villegas, J. C.; Garces, L. J.; Gomez, S.; Durand, J. P.; Suib, S. L. *Chem. Mater.* **2005**, *17* (7), 1910−1918.
(29) Zhang, Q.; Cheng, X.; Feng, X.; Qiu, G.; Tan, W.; Liu, F. *J. Mater. Chem.* **2011**, *21* (14), 5223−5225.
(30) Vacassy, R.; Scholz, S. M.; Dutta, J.; Plummer, C. J. G.; Houriet, R.; Hofmann, H. *J. Am. Ceram. Soc.* **1998**, *81* (10), 2699−2705.
(31) Wang, X.; Li, Y. *J. Am. Chem. Soc.* **2002**, *124* (12), 2880−2881.
(32) Yuan, J.; Li, W. N.; Gomez, S.; Suib, S. L. *J. Am. Chem. Soc.* **2005**, *127* (41), 14184−14185.
(33) Portehault, D.; Cassaignon, S.; Baudrin, E.; Jolivet, J.-P. *Chem. Mater.* **2007**, *19* (22), 5410−5417.
(34) Wang, Y.; Zhang, H. J.; Siah, K. W.; Wong, C. C.; Lin, J.; Borgna, A. *J. Mater. Chem.* **2011**, *21* (28), 10336−10341.
(35) Xu, K.; Hu, S.; Wu, C.; Lin, C.; Lu, X.; Peng, L.; Yang, J.; Xie, Y. *J. Mater. Chem.* **2012**, *22* (35), 18214−18220.
(36) Long, Y.; Hui, J.; Wang, P.; Hu, S.; Xu, B.; Xiang, G.; Zhuang, J.; Lu, X.; Wang, X. *Chem. Commun.* **2012**, *48* (47), 5925−5927.
(37) Long, Y.; Hui, J.; Wang, P.; Xiang, G.; Xu, B.; Hu, S.; Zhu, W.; Lü, X.; Zhuang, J.; Wang, X. *Sci. Rep.* **2012**, *2*, 612.
(38) Suib, S. L.; Iton, L. E. *Chem. Mater.* **1994**, *6* (4), 429−433.
(39) Zhang, T.; Zhang, X.; Ng, J.; Yang, H.; Liu, J.; Sun, D. D. *Chem. Commun.* **2011**, *47* (6), 1890−1892.
(40) Goncalves, R. H.; Cardoso, C. A.; Leite, E. R. *J. Mater. Chem.* **2010**, *20* (6), 1167−1172.
(41) Connell, J. W.; Crivello, J. V.; Bi, D. *J. Appl. Polym. Sci.* **1995**, *57* (10), 1251−1259.